Co-catalyst-free Photocatalytic Hydrogen Evolution with Simple Heteroleptic Iridium(III) Complexes

Govardhana Babu Bodedla,‡[a,c] Daniel Nnaemaka Tritton,‡[a] Xi Chen,[b] Jianzhang Zhao,[b] Zeling Guo,[c] Ken Cham-Fai Leung,[a,] Wai-Yeung Wong,[c,]* and Xunjin Zhu[a,]**

[a] Department of Chemistry. Hong Kong Baptist University, Waterloo Road, Kowloon Tong, Hong Kong, P. R. China.

[b] School of Chemical Engineering and State Key Laboratory of Fine Chemicals, Dalian University of Technology, Dalian 116024, P. R. China.

[c] Department of Applied Biology & Chemical Technology and Research Institute for Smart Energy, The Hong Kong Polytechnic University. Hong Kong, P. R. China and The Hong Kong Polytechnic University Shenzhen Research Institute, Shenzhen, 518057, P. R. China.

‡ G.B.B and D.N.T contributed equally to this work.

KEYWORDS. Co-catalyst-free, photocatalytic hydrogen evolution, iridium(III) complex, photostability and reductive quenching.

ABSTRACT. A simple heteroleptic iridium(III) photosensitizer, **Ir-1**, containing two 5-(trifluoromethyl)-2-phenylpyridine (C^N-CF_3) and bipyridine (N^N) ligands has for the first time been studied for co-catalyst-free photocatalytic hydrogen evolution (PHE). The complex **Ir-1** produces a hydrogen production rate (ηH_2) of 3.2 mmol g^{-1} h^{-1}, which is over 3.6-fold higher than the control complex **Ir-2** (0.9 mmol g^{-1} h^{-1}) containing bipyridine and 2-phenylpyridine ligands

without CF_3 groups. The higher ηH_2 of **Ir-1** could be ascribed to the high light-harvesting property, longer triplet electron lifetime, more appropriate driving force for accepting electrons from the sacrificial donor, which enable efficient charge separation and transfer of electrons for hydrogen evolution. Additionally, the photostability issues of **Ir-1** and **Ir-2** are addressed by the selection of suitable organic solvent/water photocatalytic systems.

INTRODUCTION

Photoactive metal complexes based on transition metals, e.g. iridium, ruthenium and copper, etc. have attracted much attention for utility as photosensitizers in artificial energy conversion systems, such as photocatalytic hydrogen evolution (PHE).[1-4] One aspect of these complexes which makes them particularly useful in photocatalytic processes is their ability to absorb visible light, thereby inducing metal-to-ligand charge-transfer states, following with charge separation and transportation.[1-6] When designing photocatalytic systems with such light-harvesting species, it is of vital importance to minimize the structural complexity of the photosensitizer (PS) and maximize its ability to absorb photons.[7-10] Amongst these types of systems, Ir(III) complexes based on bidentate N^N ligand (typically 2,2'-bipyridine) have been included due to their functional properties,[11-16] particularly since they are brilliant candidates for PHE reactions, owing to their unique photophysical properties such as long emission lifetime, good photostability and high Stokes shift.[17-24] It is well known that by controlling the nature and position of the functional substituents on the chelating ligands, the corresponding Ir(III) complexes could be manipulated in terms of their electronic and chemical properties, giving way to electrochemical versatility and tunability.[25-28] The modification of ligands to design metal complexes with certain functionalities e.g. PHE, can greatly influence the photo-redox properties and efficiency of electron transfer in the complexes. So far, various photocatalytic systems have been studied in order to investigate the

capacity of Ir(III) complexes for PHE; these systems typically consist of a mononuclear bis-cyclometalated complex, $[Ir(C^N)_2(N^N)]^+$ (where C^N = 2-phenylpyridine and N^N = 2,2'-bipyridyl), transition metal co-catalyst, sacrificial electron donor and water source to facilitate a suitable photoinduced electron transfer cycle, ultimately resulting in the reduction of hydrogen ions (H^+) to H_2.[17-28] By mimicking natural photosynthetic pathways, using systems such as those described above, we can pave the way to developing new technologies for generating H_2 as a renewable energy source in an environmentally clean, economical and efficient manner. Additionally, such Ir(III) complexes have been synthesized by relatively straightforward procedures and provide good efficacy for PHE. Despite the benefits of these systems, there are some drawbacks including the fact that they typically make use of co-catalysts based on rare precious metals such as platinum (Pt), to give the maximum efficiency in H_2 generation; this is of course costly and hence not very commercially viable.[29] In an effort to tackle this issue, some previously studied systems make use of water reduction co-catalysts based on first-row transition metals, e.g. Co and Fe, etc.[17,18,25] However, to our knowledge, no report has ever been disclosed that Ir(III) complexes could be utilized as co-catalyst-free PHE systems with comparable hydrogen production rate.

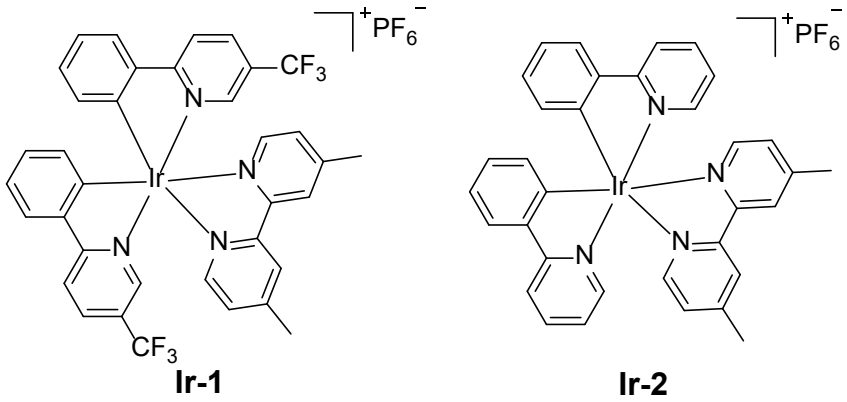

Figure 1. Structures of **Ir-1** and **Ir-2**.

Herein, we for the first time report, a simple heteroleptic Ir(III) complex, **Ir-1**, bearing 5-(trifluoromethyl)-2-phenylpyridine (C^N-CF_3) and bipyridine (N^N) ligands (Figure 1) for use as PS in PHE without the aid of a noble metal or transition metal complex as co-catalyst. For better understanding, the optoelectronic and PHE properties of **Ir-1** complex were compared to a control complex, **Ir-2** bearing 2-phenylpyridine (C^N) without CF_3 groups. When comparing the optoelectronic properties of **Ir-1** to **Ir-2**, it was found that the incorporation of CF_3 groups on C^N ligands enhances the light-harvesting property of the Ir(III) complex, stabilizing the excited triplet states and giving a greater driving force for accepting electrons from triethylamine (TEA) sacrificial donor and transfer of electrons from photoexcited triplet states to proton (H^+). As a result, a more efficient ηH_2 of 3.20 mmol g^{-1} h^{-1} was observed for **Ir-1** than for **Ir-2** (0.90 mmol g^{-1} h^{-1}).

RESULTS AND DISCUSSION

The synthesis of **Ir-1** and **Ir-2** is illustrated in Scheme S1 (See ESI†). The compounds were confirmed by spectroscopic methods including ^1H and ^{13}C NMR, and MALDI-TOF MS.

The UV-Vis absorption spectra of Ir(III) complexes recorded in acetonitrile/water (MeCN/H_2O, 2:1 v/v) solution are shown in Figure 2(a) and the corresponding data are noted in Table 1. Both complexes show three main types of peaks in the absorption spectra. The intensified absorption peaks at higher energy region (ca. 250-320 nm) are attributed to the spin-allowed ligand-centred transitions (^{1}LC, i.e., π-π* transitions of C^N-CF_3 or C^N ligands, and N^N ligands), while those observed at ca. 320-400 nm correspond to singlet inter-ligand charge-transfer (^{1}LLCT) and singlet metal-to-ligand charge-transfer transitions (^{1}MLCT). The weak absorption peaks located at lower energy region (ca. 420-500 nm) are assigned to the triplet excitations such as ^{3}LC, ^{3}LLCT, and ^{3}MLCT transitions.[30] Moreover, **Ir-1** displayed intensified absorption peaks

in comparison to **Ir-2**. This indicates that the introduction of CF_3 groups on C^N ligands enhances the probability of electronic transitions and thus light-harvesting property of **Ir-1**.

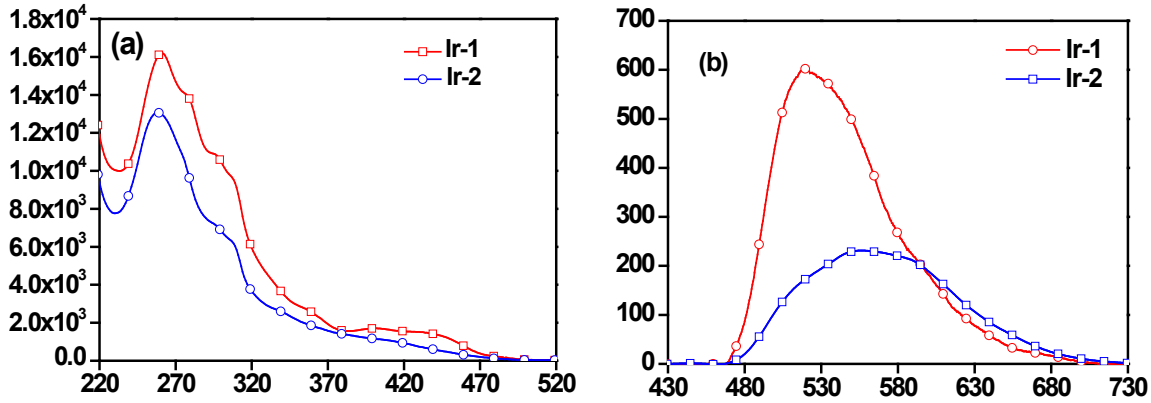

Figure 2. (a) Absorption and (b) emission spectra of **Ir-1** and **Ir-2** recorded in degassed MeCN/H_2O (2:1 v/v, 100 μM) solution at 298 K.

Table 1. Photophysical and eletrochemical data of **Ir-1** and **Ir-2**

Complex	λ_{abs}[a] ($\varepsilon/10^4$, $M^{-1}cm^{-1}$) (nm)	λ_{em}[b] (nm)	τ_{PL}[c] (μs)	τ_{PL}[d] (μs)	Φ_{PL}[e]	E_{Ox}[f] (V)	E_{Red}[f] (V)	$E_{(PS^+/PS^*)}$[g] (V)	$E_{(PS^*/PS^-)}$[h] (V)	$E_{0\text{-}0}$[i] (eV)
Ir-1	261 (1.63), 278 (1.39), 296 (1.09), 308 (0.96), 361 (0.24), 404 (0.17), 430 (0.14)	520	1.0	0.07	0.43	1.31, 1.63	–1.05 –1.61	– 1.36	1.62	2.67
Ir-2	258 (1.31), 295 (0.72), 308 (0.62), 339 (0.26), 385 (0.13), 418 (0.09)	556	0.40	0.02	0.13	1.03, 1.53	– 1.09 – 1.66	– 1.56	1.50	2.59

[a, b] Recorded in an MeCN/H_2O (2:1 v/v, 100 μM) solution. [c] Lifetime decay profile of the complexes in degassed in MeCN/H_2O (2:1 v/v, 100 μM) at 298 K. [d] Lifetime decay profile of the

complexes in aerobic MeCN/H_2O (2:1 v/v, 100 μM) at 298 K. [e] The luminescence quantum yield, measured at room temperature using $[Ru(bpy)_3]Cl_2$ in degassed MeCN/H_2O (2:1 v/v, 100 μM) solution as the reference (excitation wavelength = 436 nm, Φ_{PL} = 0.042). [f] The redox potentials of the complexes were recorded in MeCN/H_2O (2:1 v/v, 100 μM) with 0.1 M $TBAPF_6$ as electrolyte (working electrode: glassy carbon; counter electrode: Pt wire; reference electrode: non-aqueous Ag/Ag^+; ferrocene was used as internal standard for potential calibration). [g] $E_{(PS^+/PS^*)}$ (vs NHE) = $E_{Ox} - E_{0\text{-}0}$. [h] $E_{(PS^*/PS^-)}$ (vs NHE) = $E_{Red} + E_{0\text{-}0}$. [i] Estimated from the intersection of the normalized absorption and emission spectra.

Figure 2(b) shows the emission spectra of **Ir-1** and **Ir-2** in MeCN/H_2O upon excitation at 410 nm. The emission data of the complexes are summarized in Table 1. Both **Ir-1** and **Ir-2** show structureless broad emission peaks at 520 nm and 570 nm, respectively, indicating that the emission transitions are attributed to strong ^{3}MLCT character. However, **Ir-1** containing C^N-CF_3 ligands induced an intensified emission peak and 50 nm blue-shift in emission maximum (λ_{em}) compared to that of **Ir-2** lacking the CF_3 group on C^N. It could be explained by the increased HOMO-LUMO gap for **Ir-1**, which can be accounted for by the inductive electron-withdrawing CF_3 group that stabilizes and decreases the HOMO levels, thereby inducing a hypsochromically blue-shifted emission (see $E_{0\text{-}0}$ values).[31-33] This indicates that the introduction of CF_3 groups on C^N ligands has a great influence on the electronic excitations of Ir(III) complexes by increasing the HOMO-LUMO energy gap that consequently displays deep blue emission. Also, concentration dependent emissions of both complexes show no observable change in their λ_{em}, confirming the absence of any excimeric or aggregate emission (Figure S3 and S4). The quantum yield (Φ_F) of the complexes **Ir-1** and **Ir-2** were calculated to be 43% and 13%, respectively. We also calculated the electron lifetime (τ_{PL}) values of the complexes to gain more insight on their exited states

character. Figure 3(a) shows the τ_{PL} decay profile of the **Ir-1** and **Ir-2** complexes in degassed MeCN at 298 K, corresponding to their calculated τ_{PL} of 1.0 and 0.4 µs, respectively, and 0.07 and 0.02 µs, respectively in the presence of air-equilibrated conditions (Figure S5). This further proves that the emission lifetimes possess triplet character (*i.e.*, phosphorescent nature of the emission).[34] The τ_{PL} of the complexes are in good agreement with their Φ_{PL} values. The 2.5-fold higher τ_{PL} of **Ir-1** than that of **Ir-2** indicates that the introduction of CF_3 groups on C^N ligands is beneficial for longer lived photoexcited triplet states of Ir(III) complexes. The results reveal that **Ir-1** could be employed as a more efficient photosensitizer than **Ir-2** for PHE (*vide infra*).

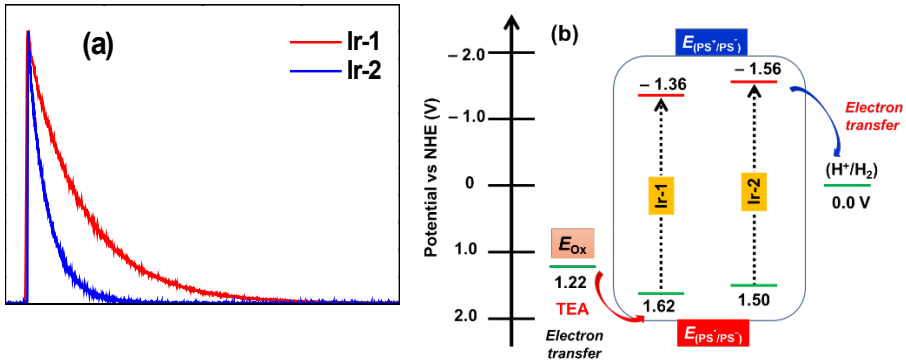

Figure 3. (a) Lifetime decay spectra of the complexes, **Ir-1** and **Ir-2** recorded in degassed MeCN/H_2O (2:1 v/v, 100 µM) at 298 K and (b) energy level allignments for thermodynamic feasibility of electron transfer between the components used in photocatalytic systems.

The HOMO and LUMO values of the complexes which corresponded to first oxidation potential (E_{Ox}) and first reduction potential (E_{Red}) values, respectvely were calculated (Table1) by recording cyclic voltammetry profiles (Figure S5). The calculated HOMO values of **Ir-1** and **Ir-2** are 1.31 and 1.03 V, respectively, whereas LUMO values of **Ir-1** and **Ir-2** are –1.05 and –1.09 V, respectively. The low-lying HOMO value for **Ir-1** (1.31 V) compared to that of **Ir-2** (1.03 V) is primarily attributed to the electron-withdrawing ability of the CF_3 groups on the C^N ligands making it more difficult to oxidize the metal center.[31, 34] On the other hand, **Ir-1** and **Ir-2** showed

similar LUMO values which could be ascribed to localization of LUMO mainly on 2,2'-bipyridine ligand. Furthermore, we also calculated the excited state oxidation ($E_{(PS^{+}/PS^{*})}$) and reduction ($E_{(PS^{*}/PS^{-})}$) potentials by using Rehm-Weller equations to estaimate the theromdynamic feasibilty of electrion transfer during the PHE cycle.[35-38] The $E_{(PS^{*}/PS^{-})}$ of **Ir-1** and **Ir-2** were calculated to be 1.62 and 1.50 V, thereby, the $E_{(PS^{+}/PS^{*})}$ were calculated to be –1.36 and –1.56 V for **Ir-1** and **Ir-2**, respectively. As seen in Figure 3(b), the $E_{(PS^{*}/PS^{-})}$ values of the complexes are more positive than the oxidation potential (E_{Ox}) of triethylamine (TEA), while the $E_{(PS^{+}/PS^{*})}$ values of complexes are more negative than the hydrogen reduction potential. This suggests a favourable thermodynamic driving force for electron transfer from TEA to photoexcited Ir-complex (PS*) and effective transfer of electrons from PS* to H^{+} ions. The relatively lower-lying $E_{(PS^{+}/PS^{*})}$ and $E_{(PS^{*}/PS^{-})}$ energy levels of **Ir-1** than **Ir-2** may increase the electron injection rate and more sufficient driving force for electron transfer from TEA to PS* and consequently expectable higher PHE efficiency (*vide infra*).[30, 31]

To gain more insight into the electronic properties of the complexes, we performed density functional theory (DFT) calculations. The geometries of the complexes were optimized at B3LYP/6-31G(d)/GENECP level by using Gaussian 09. Figure 4 shows the electronic density distribution in the frontier molecular orbitals HOMO and LUMO of the complexes. For both complexes, the HOMO is mainly contributed by the Ir atom and the C^N ligands, while the LUMO is mainly localized on the N^N ligand. This indicates that the HOMO to LUMO electronic excitation leads to migration of electrons from both the Ir atom and C^N ligands to N^N ligand under photoexcitation. Moreover, the spatial separation of the HOMO and the LUMO in both **Ir-I** and **Ir-2** complexes can lead to generation of charge-separated excited states upon photoexcitation. The well charge-separated excited states of **Ir-1** and **Ir-2** indicate that there would

be efficient charge separation and transfer of photogenerated electrons for them and therefore could be employed as efficient photosensitizers in PHE.

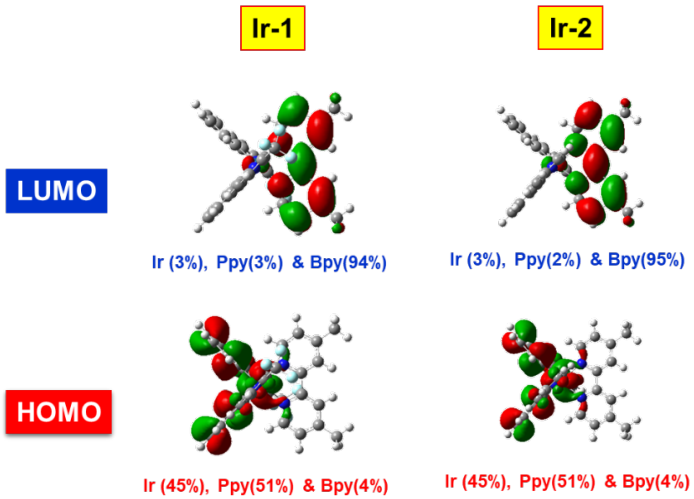

Figure 4. Calculated electronic density distribution in frontier molecular orbitals of **Ir-1** and **Ir-2**. For the sake of convenience, 2-phenylpyridine and bipyridyl ligands were represented as Ppy and Bpy respectively. Calculations were done at B3LYP/6-31G(d)/GENECP level with Gaussian 09W.

We fabricated a set of photocatalytic systems by employing **Ir-1** and **Ir-2** as PSs, TEA as sacrificial donor, water as proton source and the organic solvent MeCN for dissolving PSs and making homogeneous solution with water.[23] The PHE results of photocatalytic systems are shown in Figure 5 and the corresponding results are summarized in Table 2. The system of **Ir-1** showed a higher hydrogen production rate (ηH_2) of 3.2 mmol g^{-1} h^{-1} within 5 h of irradiation, which is over 3.6-fold higher than that of **Ir-2** (0.9 mmol g^{-1} h^{-1}). The higher hydrogen evolution of **Ir-1** than **Ir-2** could be ascribed to the following factors: (i) good light-harvesting property (ii) longer electron lifetime, (iii) suitable $E_{(PS^+/PS^*)}$ and $E_{(PS^*/PS^-)}$ energy levels for efficient complex regeneration by TEA and effective electron transfer from photoexcited states to H^+, respectively (*vide infra*) and (iv) efficient photoinduced hole-electron pairs separation and their migration

(Figure S1).[39] All these together further enhanced the transfer of electrons from photoexcited **Ir-1** to proton and consequently enhanced PHE. Since the photocatalytic systems of **Ir-1** and **Ir-2** produced the efficient PHE in the absence of co-catalysts such as Pt and Co(III) based complexes, we also tested the PHE in the absence of a sacrificial donor. Unfortunately, the photocatalytic systems did not produce any H_2, indicating that TEA is necessary to initiate the photocatalytic cycle. Moreover, we also studied the ηH_2 of photocatalytic systems in the presence of Pt co-catalyst and compared with ηH_2 of co-catalyst free photocatalytic systems to understand the reliabilty of **Ir-1** and **Ir-2** for co-catalyst free PHE. From Figure S10, it was found that **Ir-1** and **Ir-2** produced ηH_2 of 9.50 and 2.86 mmol g^{-1} h^{-1} (Table 2), respectively, which are 3-fold higher than the co-catalyst free photocatalsytic systems. This result clearly indicates that **Ir-1** and **Ir-2** are also good enough to produce H_2 in the absence of Pt co-catalyst. In order to further improve ηH_2 of photocatalytic systems, the sacrificial donors such as triethanolamine (TEOA) and ascorbic acid (AA) were tested instead of TEA. As depicted in Figure S11, the photocatalytic systems of TEOA and AA showed lower ηH_2 than TEA photocatalytic systems indicating that the use of TEA as sacrficial donor is the most suitable choice for **Ir-1** and **Ir-2** photosensitizers. Surprisingly, though several Ir(III) complexes with general structure $[Ir(C\hat{}N)_2(N\hat{}N)]^+$ have been reported for the efficient PHE so far, no one reported the PHE without using co-catalysts. This highlights that we first disclosed the co-catalyst free PHE with comparable hydrogen production rates. The PHE of the systems continuously increased from the initial time of irradiation to 20 h and afterwards showed leveling off. This could be ascribed to the degradation of Ir-complexes due to cleavage of weak dative coordinate metal-(N^N) bonds by MeCN solvent. The ESI-MS spectra of **Ir-1** and **Ir-2** also further proved their degradation (Figure S6-S9). Interstingly, it should be noted that the CF_3 groups of decomposed **Ir-1** complex were converted into CH_3 groups (Figure S7). This could be

ascribed to the nucleophilic hydride ion (which generated during the photocatalytic pathway) substitution at carbon atom of CF_3 groups and simultaneous leaving of fluoride ion. Moreover, since the homoleptic cyclometalated tris(2-phenylpyridine)iridium(III) (**Ir-3)** did not contain the metal-(N^N) bonds**,** we presumed that PHE testing of this complex can give more insight into the degradation of Ir-complexes. The photocatalytic system of **Ir-3** exhbited very low ηH_2 of 0.24 mmol g^{-1} h^{-1} and continuously increased PHE up to 50 h of light irradiation. This indicates that the strong covalent metal-(C^N) bonds of **Ir-3** restricted its degradation by MeCN solvent (Figure 6).

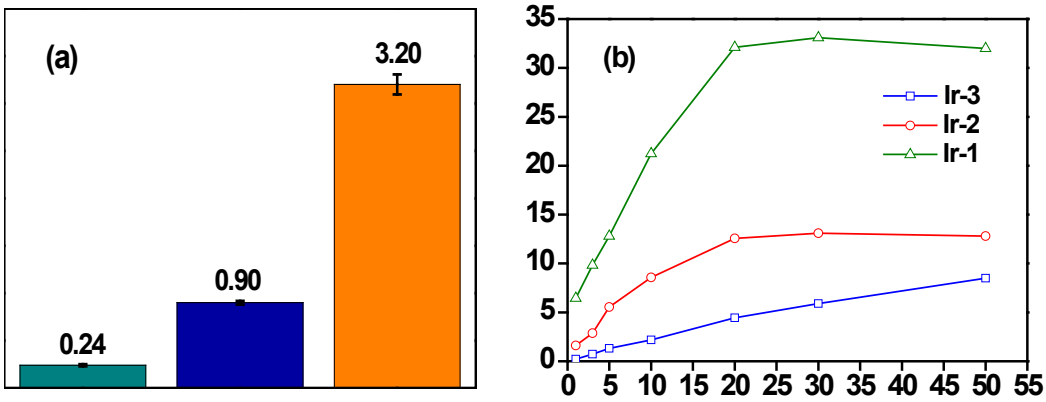

Figure 5. (a) ηH_2 of photocatalytic systems of **Ir-1, Ir-2** and **Ir-3** under irradiation for 5 h and (b) H_2 production of photocatalytic systems of **Ir-1, Ir-2** and **Ir-3** under irradiation for 50 h: PS (100 μM) + Sacrificial donor (0.8 M) + MeCN/H_2O (2:1 v/v).

Table 2. The PHE data of the photocatalytic systems

Complex	**Ir-1**[a]	**Ir-2**[a]	**Ir-3**[a]	**Ir-1**[b]	**Ir-2**[b]	**Ir-3**[b]	**Ir-1**[c]	**Ir-2**[c]	**Ir-3**[c]	**Ir-1**[d]	**Ir-2**[d]
ηH_2 (mmol g^{-1} h^{-1})	3.20	0.90	0.24	1.35	0.44	0.13	0.70	0.20	0.18	9.50	2.86
AQE	0.70	0.20	0.01	0.40	0.15	0.03	0.25	0.09	0.01	1.1	0.56

[a] ηH_2 of photocatalytic systems of **Ir-1, Ir-2** and **Ir-3** under irradiation for 5 h: PS (100 μM) + Sacrificial donor (0.8 M) + MeCN/H_2O (2:1 v/v). [b] ηH_2 of photocatalytic systems of **Ir-1, Ir-2** and **Ir-3** under irradiation for 5 h: PS (100 μM) + Sacrificial donor (0.8 M) + THF/H_2O (2:1 v/v). [c] ηH_2 of photocatalytic systems of **Ir-1, Ir-2** and **Ir-3** under irradiation for 5 h: PS (100 μM) + Sacrificial donor (0.8 M) + DMF/H_2O (2:1 v/v). [d] ηH_2 of photocatalytic systems of **Ir-1** and **Ir-2** under irradiation for 5 h: PS (100 μM) + Sacrificial donor (0.8 M) + Pt (3 wt%) + MeCN/H_2O (2:1 v/v).

In order to further prove whether the degradation of **Ir-1** and **Ir-2** was induced by the MeCN solvent, we tested their PHE in the presence of THF/H_2O and DMF/H_2O solvent systems. Though **Ir-1** and **Ir-2** showed very low ηH_2 under THF/H_2O and DMF/H_2O solvent systems compared to that of MeCN/H_2O solvent system (Figure 6(a) & (b)), they did not degrade after 50 h light irradiation and produced PHE continuously from the initial time of irradiation (Figure 6(c) and (d)). This indicates the excellent photostabilty of **Ir-1** and **Ir-2** under THF/H_2O and DMF/H_2O solvent system conditions. All these results strongly illustrate that the **Ir-1** and **Ir-2** complexes underwent photolysis under the MeCN/H_2O solvent system and thus leveled off in PHE after 20 h light irradiation. It is worth mentioning that most of the systems based on Ir(III) complexes as

sensitizers and Co(III)) based complexes as co-catalyst could drop the catalytic activity under long-term photo-irradiation. This could be attributed to the dissociation of Co(III) based complexes, which leads to the loss of catalytic activity and limited photostability of the systems.[32] The use of complexes **Ir-1** and **Ir-2** in a weakly coordinating solvent is very promising in co-catalyst free PHEs, which overcomes the photostability issue and reduces the complexity of the photocatalytic systems. The apparent quantum efficieny (AQE) of the photocatalytic systems were recorded under light irradiation at 420 nm (Table 2). The AQE values of photocatlytic systems were well matched to their ηH_2. Finally, all these results demonstrate that the incorporation of CF_3 groups to C^N ligand is beneficial to improve the PHE by enhancing the photogenerated electrons and their transfer from photo excited Ir(III) motif to proton.

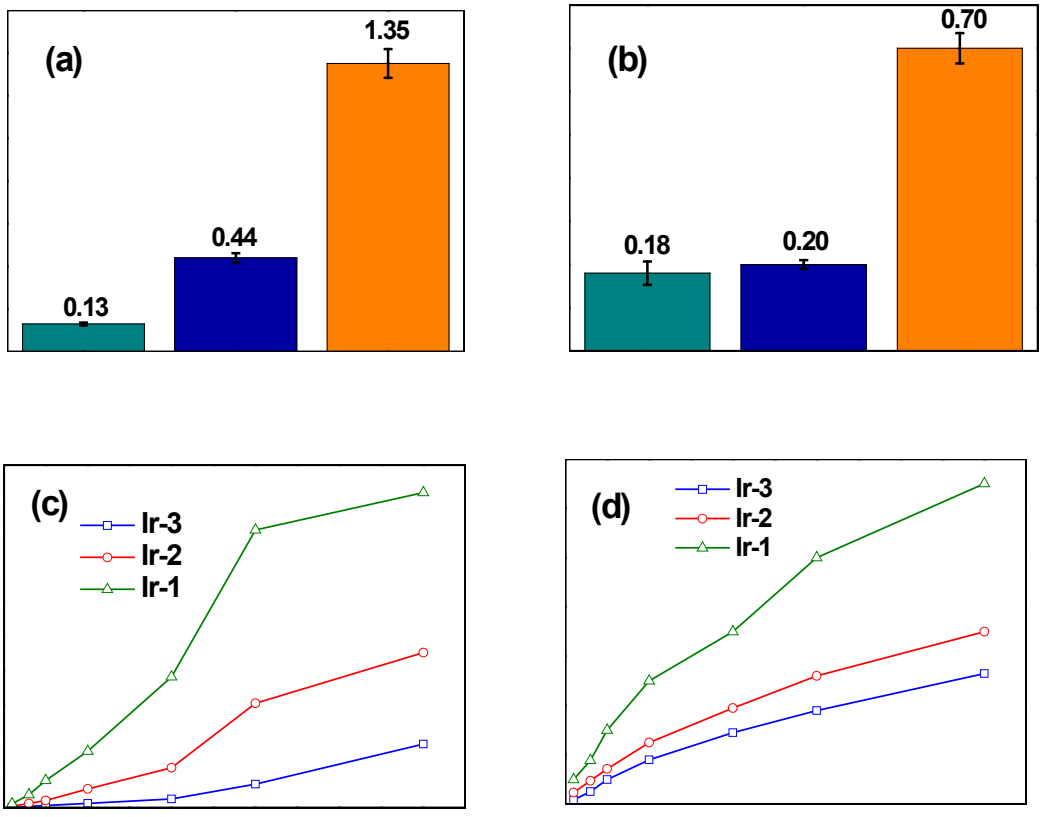

Figure 6. H_2 production rate of photocatalytic systems of **Ir-1, Ir-2** and **Ir-3** under irradiation for 5 h (a) PS (100 μM) + Sacrificial donor (0.8 M) + THF/H_2O (2:1 v/v and (b) PS (100 μM) + Sacrificial donor (0.8 M) + DMF/H_2O (2:1 v/v), H_2 production of photocatalytic systems of **Ir-1, Ir-2** and **Ir-3** under irradiation for 50 h and (c) PS (100 μM) + Sacrificial donor (0.8 M) + THF/H_2O (2:1 v/v) and (d) PS (100 μM) + Sacrificial donor (0.8 M) + DMF/H_2O (2:1 v/v).

The phosphorescence quenching experiments of **Ir-1** and **Ir-2** were performed by varying the concentration of TEA to study the electron transfer mechanism of their PHE system (Figure S12). The Stern-Volmer quenching constants (K_q) of **Ir-1** and **Ir-2** by TEA were found to be 18.2 and 5.9 M^{-1}, respectively (Figure 7(a)), indicating that the photoexcited **Ir-1** complex could accept an electron from TEA more efficiently than **Ir-2** under photoexcitation. This result is also in good agreement with a more favourable thermodynamic driving force for electron transfer from TEA to photoexcited **Ir-1** complex (*vide supra*) and thus higher ηH_2 of **Ir-1** than **Ir-2**. Based on the phosphorescence quenching studies, $E_{(PS^+/PS^*)}$ and $E_{(PS^*/PS^-)}$ energy levels and PHE results, we deduced that the photocatalytic pathway of **Ir-1** and **Ir-2** could be assigned to the reductive quenching mechanism (Figure 7(b)). In this process, firstly, the Ir complex absorbs light and is photoexcited to an excited state. Secondly, the excited Ir-complex accepts an electron from TEA to produce a reduced Ir complex species, which can donate an electron directly to proton and then relaxes back down to the ground state. Finally, the repeated photocycles produce H_2.[35, 36, 37]

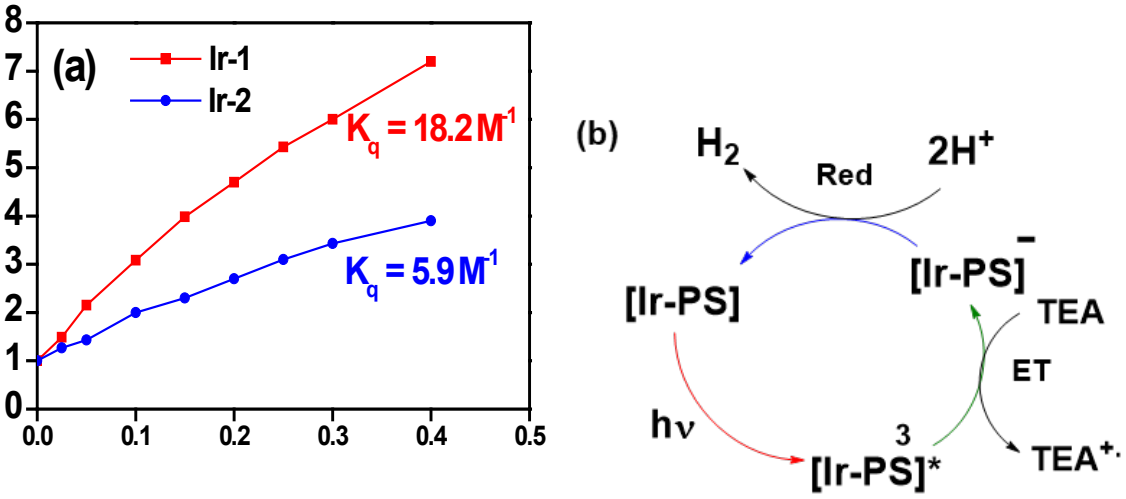

Figure 7. (a) Stern-Volmer plot of **Ir-1** and **Ir-2** in MeCN/H_2O (2:1 v/v, 100 μM) with TEA as quencher and (b) proposed electron transfer mechanism and photo-redox cycle for PHE with Ir-PS (**Ir-1** and **Ir-2**). PS is photosensitizer, ET is electron transfer and Red is reduction.

CONCLUSIONS

In conclusion, we synthesized a simple heteroleptic Iridium(III) photosensitizer, **Ir-1** by incorporating CF_3 groups on the C^N ligands and compared its optoelectronic and PHE properties to the control complex **Ir-2** without CF_3 groups. Optoelectronic and transient photocurrent response spectra studies revealed that **Ir-1** possesses a higher light-harvesting property, long-lived photo-excited triplet states and enhanced photoinduced charge separation than that of **Ir-2**. The phosphorescence quenching experiments revealed that the photoexcited **Ir-1** complex could accept an electron from TEA more efficiently than the **Ir-2** under photoexcitation. As a result, the photocatalytic system of **Ir-1** exhibited efficient PHE without the use of a water reduction co-catalyst. **Ir-1** showed ηH_2 of 3.20 mmol g^{-1} h^{-1}, which was over 3.6-fold higher than the control complex **Ir-2** (0.90 mmol g^{-1} h^{-1}) and much higher than the homoleptic **Ir-3** complex (0.24 mmol

g^{-1} h^{-1}). Moreover, the Ir-complexes showed a comparable ηH_2 in THF/H_2O or DMF/H_2O systems, representing the most photostable co-catalyst-free PHE system reported to date.

Supporting Information

Supporting Information file contains the following contents: Materials and methods, synthesis, cyclic voltammograms, ^1H and ^{13}C NMR spectra, MALDI–TOF spectrum.

AUTHOR INFORMATION

Corresponding Author

* X. Zhu, E-mail: xjzhu@hkbu.edu.hk

* Ken Cham-Fai Leung *cfleung@hkbu.edu.hk*

* Wai-Yeung Wong: wai-yeung.wong@polyu.edu.hk

Notes

There are no conflicts to declare.

ACKNOWLEDGMENT

The research was supported by Hong Kong Research Grants Council (HKBU 12304320). K.C.-F Leung thanks the State Key Laboratory of Environmental and Biological Analysis as well as The President's Award for Outstanding Performance in Research Supervision to K.C.-F.L.. W.-Y. Wong. acknowledges the financial support from Hong Kong Research Grants Council (PolyU 153058/19P), the National Natural Science Foundation of China (51873176), the Hong Kong Polytechnic University (1-ZE1C), Ms. Clarea Au for the Endowed Professorship in Energy (847S) and the Research Institute for Smart Energy (RISE)

REFERENCES

1. Yuan, Y.-J.; Yu, Z.-T.; Chen, D.-Q.; Zou, Z.-G. Metal-complex Chromophores for Solar Hydrogen Generation. *Chem. Soc. Rev.* **2017,** *46* (3), 603-631.

2. Wang, M.; Na, Y.; Gorlov, M.; Sun, L. Light-driven Hydrogen Production Catalysed by Transition Metal Complexes in Homogeneous Systems. *Dalton Trans.* **2009,** (33), 6458-6467.

3. Frischmann, P. D.; Mahata, K.; Würthner, F. Powering the Future of Molecular Artificial Photosynthesis with Light-harvesting Metallosupramolecular Dye Assemblies. *Chem. Soc. Rev.* **2013,** *42* (4), 1847-1870.

4. Yu, J.; He, Q.; Yang, G.; Zhou, W.; Shao, Z.; Ni, M. Recent Advances and Prospective in Ruthenium-Based Materials for Electrochemical Water Splitting. *ACS Catal.* **2019,** *9* (11), 9973-10011.

5. Huang, T.; Yu, Q.; Liu, S.; Huang, W.; Zhao, Q. Phosphorescent Iridium(iii) Complexes: A Versatile Tool for Biosensing and Photodynamic Therapy. *Dalton Trans.* **2018,** *47* (23), 7628-7633.

6. Stacey, O. J.; Pope, S. J. A. New Avenues in the Design and Potential Application of Metal Complexes for Photodynamic Therapy. *RSC Adv.* **2013,** *3* (48), 25550-25564.

7. Kaeffer, N.; Chavarot-Kerlidou, M.; Artero, V. Hydrogen Evolution Catalyzed by Cobalt Diimine–Dioxime Complexes. *Acc. Chem. Res.* **2015,** *48* (5), 1286-1295.

8. Zhang, P.; Wang, M.; Na, Y.; Li, X.; Jiang, Y.; Sun, L. Homogeneous Photocatalytic Production of Hydrogen from Water by a Bioinspired [Fe_2S_2] Catalyst with High Turnover Numbers. *Dalton Trans.* **2010,** *39* (5), 1204-1206.

9. Li, X.; Wang, M.; Zheng, D.; Han, K.; Dong, J.; Sun, L. Photocatalytic H_2 Production in Aqueous Solution with Host-guest Inclusions Formed by Insertion of an FeFe-hydrogenase Mimic and An Organic Dye into Cyclodextrins. *Energy Environ. Sci.* **2012,** *5* (8), 8220-8224.

10. Wenger, O. S. Long-range Electron Transfer in Artificial Systems with d_6 and d_8 Metal Photosensitizers. *Coord. Chem. Rev.* **2009,** *253* (9), 1439-1457.

11. Majumdar, P.; Yuan, X.; Li, S.; Le Guennic, B.; Ma, J.; Zhang, C.; Jacquemin, D.; Zhao, J. Cyclometalated Ir(III) Complexes with Styryl-BODIPY Ligands Showing Near IR Absorption/emission: Preparation, Study of Photophysical Properties and Application as Photodynamic/luminescence Imaging Materials. *J. Mater. Chem. B* **2014,** *2* (19), 2838-2854.

12. Brooks, A. C.; Basore, K.; Bernhard, S. Photon-Driven Reduction of Zn^{2+} to Zn Metal. *Inorg. Chem.* **2013,** *52* (10), 5794-5800.

13. You, Y.; Nam, W., Photofunctional Triplet Excited States of Cyclometalated Ir(III) Complexes: Beyond Electroluminescence. *Chem. Soc. Rev.* **2012,** *41* (21), 7061-7084.

14. Ma, Y.; Liang, H.; Zeng, Y.; Yang, H.; Ho, C.-L.; Xu, W.; Zhao, Q.; Huang, W.; Wong, W.-Y., Phosphorescent Soft Salt for Ratiometric and Lifetime Imaging of Intracellular pH Variations. *Chem. Sci.* **2016,** *7* (5), 3338-3346.

15. Sun, H.; Liu, S.; Lin, W.; Zhang, K. Y.; Lv, W.; Huang, X.; Huo, F.; Yang, H.; Jenkins, G.; Zhao, Q.; Huang, W. Smart Responsive Phosphorescent Materials for Data Recording and Security Protection. *Nat. Commun.* **2014,** *5* (1), 3601.

16. Chen, Z.-q.; Bian, Z.-q.; Huang, C.-h., Functional Ir(III) Complexes and Their Applications. *Adv. Mater.* **2010,** *22* (13), 1534-1539.

17. Lentz, C.; Schott, O.; Auvray, T.; Hanan, G. S.; Elias, B. Design and Photophysical Studies of Iridium(III)–cobalt(III) Dyads and Their Application for Dihydrogen Photo-evolution. *Dalton Trans.* **2019,** *48* (41), 15567-15576.

18. Gärtner, F.; Denurra, S.; Losse, S.; Neubauer, A.; Boddien, A.; Gopinathan, A.; Spannenberg, A.; Junge, H.; Lochbrunner, S.; Blug, M.; Hoch, S.; Busse, J.; Gladiali, S.; Beller,

M. Synthesis and Characterization of New Iridium Photosensitizers for Catalytic Hydrogen Generation from Water. *Chem. Eur. J* **2012,** *18* (11), 3220-3225.

19. Goldsmith, J. I.; Hudson, W. R.; Lowry, M. S.; Anderson, T. H.; Bernhard, S. Discovery and High-Throughput Screening of Heteroleptic Iridium Complexes for Photoinduced Hydrogen Production. *J. Am. Chem. Soc.* **2005,** *127* (20), 7502-7510.

20. Cline, E. D.; Adamson, S. E.; Bernhard, S. Homogeneous Catalytic System for Photoinduced Hydrogen Production Utilizing Iridium and Rhodium Complexes. *Inorg. Chem.* **2008,** *47* (22), 10378-10388.

21. Yuan, Y.-J.; Yu, Z.-T.; Chen, X.-Y.; Zhang, J.-Y.; Zou, Z.-G. Visible-Light-Driven H_2 Generation from Water and CO_2 Conversion by Using a Zwitterionic Cyclometalated Iridium(III) Complex. *Chem. Eur. J.* **2011,** *17* (46), 12891-12895.

22. Yu, Z.-T.; Yuan, Y.-J.; Cai, J.-G.; Zou, Z.-G. Charge-Neutral Amidinate-Containing Iridium Complexes Capable of Efficient Photocatalytic Water Reduction. *Chem. Eur. J.* **2013,** *19* (4), 1303-1310.

23. Tritton, D. N.; Bodedla, G. B.; Tang, G.; Zhao, J.; Kwan, C.-S.; Leung, K. C.-F.; Wong, W.-Y.; Zhu, X., Iridium Motif Linked Porphyrins for Efficient Light-driven Hydrogen Evolution via Triplet state Stabilization of Porphyrin. *J. Mater. Chem. A* **2020,** *8* (6), 3005-3010.

24. Cai, J.-G.; Yu, Z.-T.; Yuan, Y.-J.; Li, F.; Zou, Z.-G. Dinuclear Iridium(III) Complexes Containing Bibenzimidazole and Their Application to Water Photoreduction. *ACS Catal.* **2014,** *4* (6), 1953-1963.

25. Lentz, C.; Schott, O.; Auvray, T.; Hanan, G.; Elias, B. Photocatalytic Hydrogen Production Using a Red-Absorbing Ir(III)–Co(III) Dyad. *Inorg. Chem.* **2017,** *56* (18), 10875-10881.

26. DiSalle, B. F.; Bernhard, S. Orchestrated Photocatalytic Water Reduction Using Surface-Adsorbing Iridium Photosensitizers. *J. Am. Chem. Soc.* **2011,** *133* (31), 11819-11821.

27. Tinker, L. L.; McDaniel, N. D.; Curtin, P. N.; Smith, C. K.; Ireland, M. J.; Bernhard, S. Visible Light Induced Catalytic Water Reduction without an Electron Relay. *Chem. Eur. J.* **2007,** *13* (31), 8726-8732.

28. Fihri, A.; Artero, V.; Pereira, A.; Fontecave, M. Efficient H_2-producing Photocatalytic Systems Based on Cyclometalated Iridium- and Tricarbonylrhenium-diimine Photosensitizers and Cobaloxime Catalysts. *Dalton Trans.* **2008,** (41), 5567-5569.

29. Whang, D. R.; Sakai, K.; Park, S. Y. Highly Efficient Photocatalytic Water Reduction with Robust Iridium(III) Photosensitizers Containing Arylsilyl Substituents. *Angew. Chem. Int. Ed.* **2013,** *52* (44), 11612-11615.

30. Fan, S.; Zong, X.; Shaw, P. E.; Wang, X.; Geng, Y.; Smith, A. R. G.; Burn, P. L.; Wang, L.; Lo, S.-C. Energetic Requirements of Iridium(III) Complex Based Photosensitisers in Photocatalytic Hydrogen Generation. *Phys. Chem. Chem. Phys.* **2014,** *16* (39), 21577-21585.

31. Lowry, M. S.; Goldsmith, J. I.; Slinker, J. D.; Rohl, R.; Pascal, R. A.; Malliaras, G. G.; Bernhard, S. Single-Layer Electroluminescent Devices and Photoinduced Hydrogen Production from an Ionic Iridium(III) Complex. *Chem. Mater.* **2005,** *17* (23), 5712-5719.

32. Tao, P.; Zhang, Y.; Wang, J.; Wei, L.; Li, H.; Li, X.; Zhao, Q.; Zhang, X.; Liu, S.; Wang, H.; Huang, W. Highly Efficient Blue Phosphorescent Iridium(iii) Complexes with Various Ancillary Ligands for Partially Solution-processed Organic Light-emitting Diodes. *J. Mater. Chem. C* **2017,** *5* (36), 9306-9314.

33. Ham, H. W.; Jung, K. Y.; Kim, Y. S. Synthesis and Photophysical Studies of Blue Phosphorescent Ir(III) Complexes with Dimethylphenylphospine. *J. Nanosci. Nanotechnol.* **2012,** *12* (2), 1265-70.

34. Yuan, Y.-J.; Yu, Z.-T.; Gao, H.-L.; Zou, Z.-G.; Zheng, C.; Huang, W. Tricyclometalated Iridium Complexes as Highly Stable Photosensitizers for Light-Induced Hydrogen Evolution. *Chem. Eur. J* **2013,** *19* (20), 6340-6349.

35. Guo, S.; Chen, K.-K.; Dong, R.; Zhang, Z.-M.; Zhao, J.; Lu, T.-B. Robust and Long-Lived Excited State Ru(II) Polyimine Photosensitizers Boost Hydrogen Production. *ACS Catal.* **2018,** *8* (9), 8659-8670.

36. Zhang, N.; Chen, K.-K.; Guo, S.; Wang, P.; Zhang, M.; Zhao, J.; Zhang, Z.-M.; Lu, T.-B. Sensitizing Ru(II) Polyimine Redox Center with Strong Light-harvesting Coumarin Antennas to Mimic Energy Flow of Biological Model for Efficient Hydrogen Evolution. *Appl. Catal. B* **2019,** *253*, 105-110.

37. Yang, M.; Yarnell, J. E.; El Roz, K.; Castellano, F. N., A Robust Visible-Light-Harvesting Cyclometalated Ir(III) Diimine Sensitizer for Homogeneous Photocatalytic Hydrogen Production. *ACS Appl. Energy Mater.* **2020,** *3* (2), 1842-1853.

38. Vlcek, A. A.; Dodsworth, E. S.; Pietro, W. J.; Lever, A. B. P. Excited State Redox Potentials of Ruthenium Diimine Complexes; Correlations with Ground State Redox Potentials and Ligand Parameters. *Inorg. Chem*. **1995**, *34* (7), 1906-1913.

39. Pan, Y.; Qian, Y.; Zheng, X.; Chu, S.-Q.; Yang, Y.; Ding, C.; Wang, X.; Yu, S.-H.; Jiang, H.-L. Precise Fabrication of Single-atom Alloy Co-catalyst with Optimal Charge State for Enhanced Photocatalysis. *Natl. Sci. Rev*. **2021,** *8* (1), nwaa224 (1-8).

Table of Contents

A heteroleptic iridium(III) photosensitizer was disclosed for co-catalyst-free highly efficient photocatalytic hydrogen evolution.

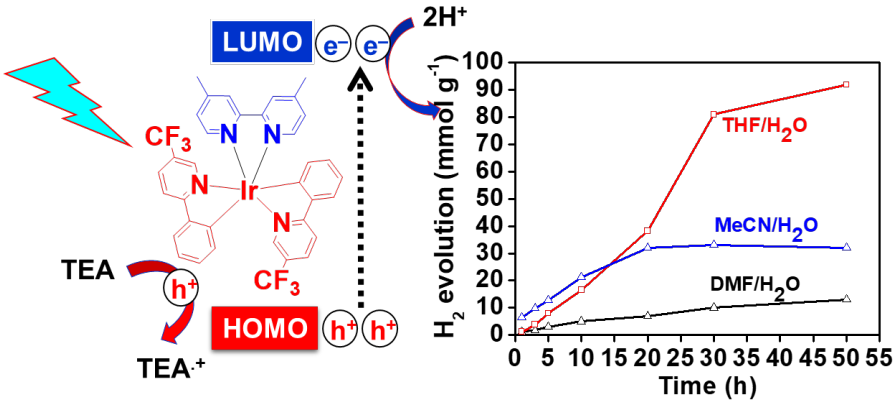

Water Reduction Catalyst Free Photocatalytic Hydrogen Evolution